An AC Resistance Optimization Method Applicable for Inductor and Transformer Windings with Full Layers and Partial Layers

Shen, Zhan; Li, Zhiguang; Jin, Long; Wang, Huai

Published in:
Proceedings of the 2017 IEEE Applied Power Electronics Conference and Exposition (APEC)

DOI (link to publication from Publisher):
10.1109/APEC.2017.7931055

Publication date:
2017

Document Version
Accepted author manuscript, peer reviewed version

An AC Resistance Optimization Method Applicable for Inductor and Transformer Windings with Full Layers and Partial Layers

Zhan Shen*‡, Zhiguang Li†, Long Jin‡, and Huai Wang*
Franciszhan_shen@163.com, zhiguang-li@sac-china.com, jinlong@seu.edu.cn, hwa@et.aau.dk
*Department of Energy Technology, Aalborg University, Aalborg, Denmark
†Guodian Nanjing Automation Co., Ltd, Nanjing, China
‡School of Electrical Engineering, Southeast University, Nanjing, China

***Abstract*—This paper proposes an ac resistance optimization method applicable for both inductor and transformer windings with full layers and partial layers. The proposed method treats the number of layers of the windings as a design variable instead of as a predefined parameter, compared to existing methods. The window height and width of magnetic cores and the insulation requirements are introduced as boundary conditions in the optimization process. The optimization can be realized simply by mathematical design map analyses instead of iteration programs. Moreover, a corresponding closed form expression of ac resistance of windings with partial layers is proposed. The developed analytical equation is verified by both Finite Element Method (FEM) simulations and experimental results from two transformer prototypes. A case study of a transformer design with partial layer windings for a LCC resonant circuit is presented with experimental verifications to demonstrate the optimization method.**

***Keywords*—Magnetic components, ac resistance optimization, partial layer windings.**

I. Introduction

Medium or high frequency transformers contribute considerable power losses in power electronic converters, which become a great challenge in energy conversion efficiency. The reduction of losses in power transformers relies on both magnetic core and winding design [1–4]. Based on various analytical expressions of transformer ac resistance [5–10], the optimization of the conductor diameter for different winding types are achieved by predefined number of winding layers m, number of strands of Litz wires k_{str}, and current waveforms [11–13]. Those methods could be easily realized by simple analytical formulas, however, the required information such as m and k_{str} are difficult to be determined at the beginning of the winding optimization. One method has been proposed in [14] by introducing the restriction of core height. However, it requires program iteration and cannot reach the overall optimization in special conditions, such as a partial layer winding. The partial layer is usually the last layer of a winding and does not have the full height like other full layers, as is illustrated in Fig. 1. The magnetic field strength due to the skin and proximity effects of the partial layer is different from that of full layer. Until now, the analytical equation for ac resistance of partial layer windings is not available.

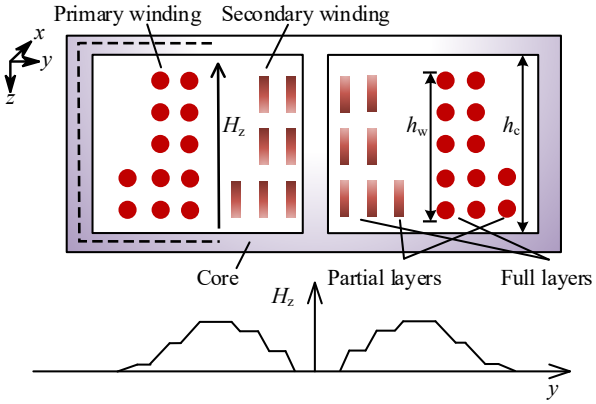

Figure 1. Cross section and magnetic field intensity distribution of transformer with partial layer windings.

In this paper, a winding design method for full layer winding is firstly proposed, which is based on the restriction of core structure and does not require to define the number of layers m. An ac resistance calculation formula for the partial layer winding is derived and verified by both FEM and experimental results, making it possible to apply the proposed optimization method to also windings with partial layers. Theoretical analyses and experimental results of a case study are also presented.

II. Optimal Winding Design with Full Layers

In this section, the one dimensional Dowell's equation along with its derivation assumptions are firstly reviewed. The conventional optimum diameter formula is then introduced and further developed to the proposed winding design method.

A. Dowell's Equation for Winding Resistance with Full Layers

Dowell's equation for ac resistance calculation is originally derived from foil and rectangle conductors. It is based on the

following assumptions for the one dimensional flux distribution [5].

- The permeability of the magnetic core is very large, so the magnetic field strength H in the core is close to zero.
- The current flows one dimension in x-direction, thus H is also one dimension in zy-plane, cf. Fig. 1.
- The height of one full layer of conductors h_{w} equals to the height of the window h_{c}, so the magnetic flux is parallel to the conductor, only in z-direction.

Based on the assumptions, the one dimensional equation for the winding ac resistance R_{ac} is given by [5]:

$$R_{\mathrm{ac}} = R_{\mathrm{dc}} F_{\mathrm{r}}, \tag{1}$$

with

$$F_{\mathrm{r}} = \triangle[\nu_3 + \frac{2}{3}(m^2 - 1)\nu_2] \tag{2}$$

and

$$\nu_2 = \frac{\sinh\triangle - \sin\triangle}{\cosh\triangle + \cos\triangle}, \quad \nu_3 = \frac{\sinh(2\triangle) + \sin(2\triangle)}{\cosh(2\triangle) - \cos(2\triangle)}, \tag{3}$$

where R_{dc} is the winding dc resistance, F_{r} is the ac resistance factor, m is the number of layers, and υ_3, υ_2 are the skin and proximity effects coefficients, separately. The ac resistance formula is the function of m and Δ, and the latter is the penetration ratio defined by:

$$\Delta = \frac{d_{\mathrm{w}}}{\delta} = d_{\mathrm{w}}\sqrt{\pi\mu f\sigma}, \tag{4}$$

where d_{w} is the thickness of conductor, δ is the skin depth, f is the frequency, and μ, σ are the permeability and conductivity of the conductor material, respectively. There is a positive correlation between Δ and frequency, meaning that the ac resistance increases with the increase of frequency for a given conductor thickness.

Dowell's equation for foil can be transferred to the rectangle and square conductor with equivalent thickness, and further to round conductor by introducing the equivalent d_{w} using equivalent area principle with the square conductor:

$$d_{\mathrm{w}} = \sqrt{\frac{\pi}{4}}d, \tag{5}$$

where d is the diameter of the round conductor.

B. Optimum Diameter Formula for Foil Conductors

It is already proved that for each particular m, there is an optimum Δ_{opt} which leads to the minimization of the total ac resistance with Dowell's equation [11–13]:

$$\Delta_{\mathrm{opt}} = \frac{1}{\sqrt[4]{\Psi}}\sqrt{\tau}, \tag{6}$$

with

$$\Psi = \frac{5m^2 - 1}{15}, \quad \text{and} \quad \tau = \frac{\omega I_{\mathrm{rms}}}{I'_{\mathrm{rms}}}, \tag{7}$$

where ω is the circular frequency, I_{rms} and I'_{rms} are the rms value of the current and the derivation of the current, respectively.

C. Winding Design for Round Conductors of Full Layers

For round conductors, the minimum resistance also exists and Δ_{opt} can be calculated by (6). Δ_{opt} for each m is given in Fig. 2 with black line. Further, the optimum diameter d can be obtained from (5) [1].

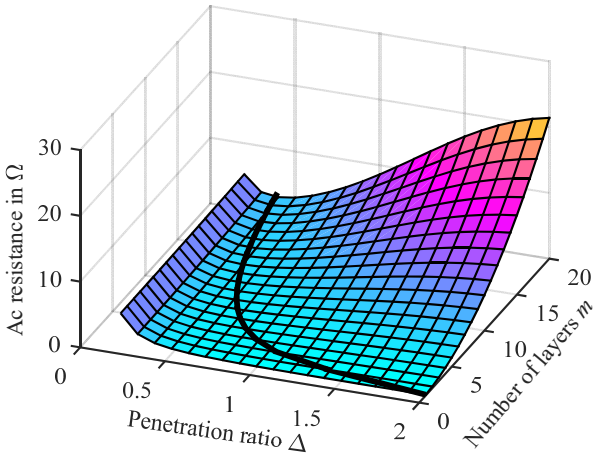

Figure 2. Ac resistance versus Δ and m with round conductor.

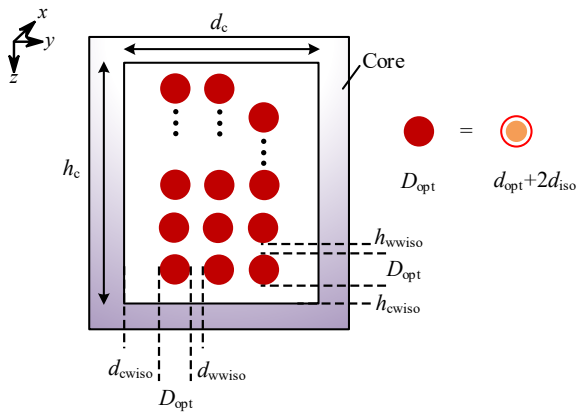

Figure 3. Transformer winding design restrictions.

In conventional inductor or transformer design process, the winding design is followed by the selection or dimension optimization of its magnetic core, thus the number of turns N is pre-determined, but not the number of layers m. For foil conductors, m equals to N and Δ_{opt} can be calculated by (6). However, for round conductors, the relationship is not valid any more and m is difficult to determine before winding design.

The proposed winding design method for round conductors is based on the dimension of the presupposed magnetic core, including two basic restrictions regarding to the width and height of the core window, as illustrated in Fig. 3:

$$d_{\mathrm{c}} \geq m d_{\mathrm{opt}} + 2m d_{\mathrm{iso}} + (m-1)d_{\mathrm{wwiso}} + 2d_{\mathrm{cwiso}}, \tag{8}$$

$$h_{\mathrm{c}} \geq t d_{\mathrm{opt}} + 2t d_{\mathrm{iso}} + (t-1)h_{\mathrm{wwiso}} + 2h_{\mathrm{cwiso}}, \tag{9}$$

where d_{c}, h_{c} is the width and height of window, t is the number of conductors of full layer in vertical direction, d_{opt} is the optimum conductor diameter, $d_{\mathrm{iso}} = p d_{\mathrm{opt}}$ is the isolation

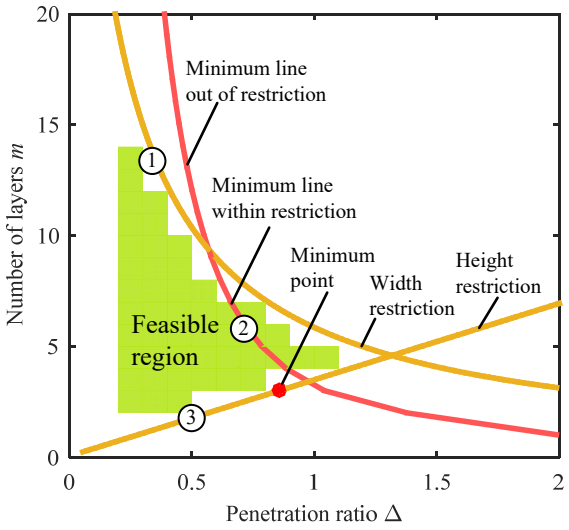

Figure 4. Transformer winding design map with full layer.

thickness of each conductor, p is the isolation coefficient, d_{wwiso}, h_{wwiso} is the isolation distance between layers in width and height direction, d_{cwiso}, h_{cwiso} is the isolation distance between core and winding in width and height direction, respectively. In full layer scenario, t is expressed by:

$$t = \frac{N}{m}. \tag{10}$$

By substituting (10) into (9) and putting them in the (Δ, m) two dimensional coordinate plane, the two restrictions can be described by the yellow line in Fig. 4. Within the restrictions all points are in feasible region, otherwise in infeasible region. The feasible region is covered with the green color. Due to the integer number of layers m, the edge of the region is not smooth and have step changes in y-axis direction. The pink line of original optimum diameter calculation is also given, with the restrictions some parts of the line is not valid any more. Notice that m axis begins from 1, which is also a restriction for the winding design.

Considering the valley shape of ac resistance in Fig. 2, the minimum ac resistance solution should be located on the boundary of the feasible region or the minimum losses line within restrictions, consisting line ①, ② and ③. The overall minimum point can be found by searching the points in the new line, as is marked with red point in the map. The method is also suitable for rectangle and square conductors by simply modifying some variables in (8) and (9).

III. Ac Windings Resistance of Partial Layers

For windings with partial layers, Dowell's equation is not valid any more. In this section, a new equation of partial layer for rectangle conductors is derived and then extended to square and round conductors. The derivation process is inspired by Dowell's equation, and is also based on the one-dimensional flux distribution assumptions. The equation is verified by both FEM simulation and experimental results.

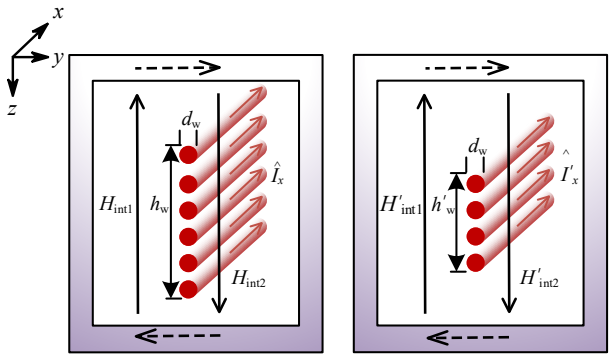

Figure 5. Magnetic boundary conditions for skin effect, left: full layer scenario, right: partial layer scenario.

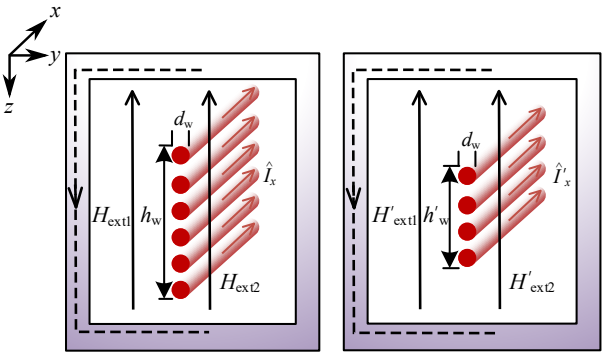

Figure 6. Magnetic boundary conditions for proximity effect, left: full layer scenario, right: partial layer scenario.

A. Equation for Winding Resistance with Partial Layers

Assuming a winding with m full layers, the partial layer is the $(m+1)th$ layer, the height of the full and partial layer h_{w} and h'_{w} can be represented by:

$$h_{\mathrm{w}} = t h_{\mathrm{w0}}, \tag{11}$$

$$h'_{\mathrm{w}} = t_0 h_{\mathrm{w0}}, \tag{12}$$

where h_{w0} is the height of single conductor, t and t_0 are the number of conductors of full and partial layer, respectively.

Define $\hat{I}_0$ as the peak current in each turn. The peak current in the full layer $\hat{I}$ is the sum of total $\hat{I}_0$ in the layer:

$$\hat{I} = t \cdot \hat{I}_0, \tag{13}$$

it decreases linearly to $\hat{I}'$ in the partial layer:

$$\hat{I}' = \frac{t_0}{t} \cdot \hat{I}. \tag{14}$$

The partial coefficient is defined as k:

$$k = \frac{t_0}{t} = \frac{h'_{\mathrm{w}}}{h_{\mathrm{w}}}. \tag{15}$$

The magnetic boundary condition for skin effect is illustrated in Fig. 5. The magnetomotive force (MMF) of partial layer is proportional to the current and decreases with the height of the partial layer. However, the magnetic flux length h_{c} does not decrease due to the one dimensional flux dis-

tribution assumption in section (II-A). As a consequence, the internal magnetic strength decreases with the partial coefficient k:

$$H'_{\mathrm{int1}} = -H'_{\mathrm{int2}} = \frac{\hat{I}'}{2h_{\mathrm{c}}} = \frac{\hat{I}}{2h_{\mathrm{c}}}\frac{h'_{\mathrm{w}}}{h_{\mathrm{w}}} = \frac{k\hat{I}}{2h_{\mathrm{c}}}. \quad (16)$$

Likewise, the boundary condition for the proximity effect is illustrated in Fig. 6. The averaged external magnetic strength boundary is:

$$H'_{\mathrm{ext1}} = H'_{\mathrm{ext2}} = \frac{\frac{m\hat{I}}{h_{\mathrm{c}}} + \frac{m\hat{I}+k\hat{I}}{h_{\mathrm{c}}}}{2} = \frac{2m\hat{I}+k\hat{I}}{2h_{\mathrm{c}}}. \quad (17)$$

By substituting these two boundary conditions of magnetic strength into the derivation process, the proposed ac resistance of round conductor transformer with m full layers and one partial layer is:

$$R_{\mathrm{ac}} = R_{\mathrm{dc}}F_{\mathrm{r}}, \quad (18)$$

with

$$F_{\mathrm{r}} = \Delta\nu_3 + \frac{4m^3 - 4m - 3k + 3k(2m+k)^2}{6(m+k)}\Delta\nu_2. \quad (19)$$

The detailed derivation process is given in Appendix A. If $k = 0$, the partial layer is disappeared and (18) turns to the Dowel's equation for m layers R_m. If $k = 1$, the partial layer becomes the additional full layer and (18) turns to the Dowell's equation for $m+1$ layers R_{m+1}. The value of (18) is between R_m and R_{m+1}. The Dowell's porosity factor η is defined by:

$$\eta = \frac{h_{\mathrm{w}}}{h_{\mathrm{c}}}. \quad (20)$$

It is used to modify the ac resistance through the penetration ratio:

$$\Delta = \sqrt{\eta}\frac{d_{\mathrm{w}}}{\delta} \quad (21)$$

to acquire a more precise analytical calculation result [5]. It also suits for the partial layer situation here.

For comparison, the ac resistance of windings with 1.56 mm diameter round conductors of full or partial layers are calculated and compared in Fig. 7. PQ 50/50 core is chosen and the length of each turn l_{w} is 94.25 mm, the operation frequency is 20 kHz. The number of layers m is 5 and the number of conductors in the full layer t is set as 10, the number of partial layer conductors t_0 increases one by one. When $t_0 = 10$, the partial layer becomes a full layer and m adds 1. In this case, the additional losses are almost 50% higher than original value when t_0 is large. It implies that compared to the proposed equation, it could have considerable errors to apply Dowell's equation to model the ac resistance of a partial layer winding. The ac resistance increment with t_0 is also not lineal according to k due to the high frequency character of skin and proximity effects.

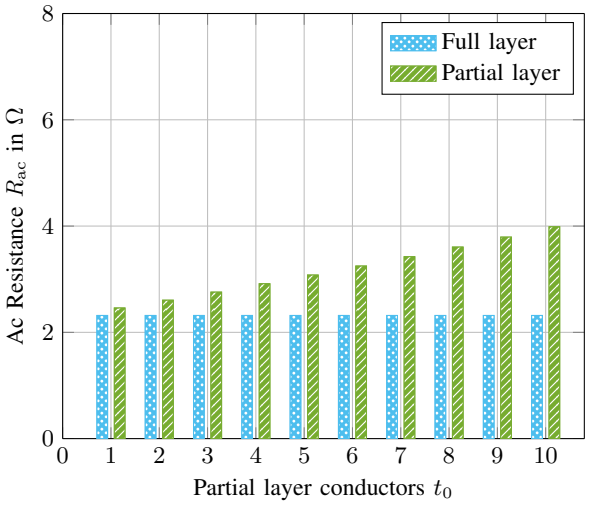

Figure 7. Comparison of ac resistance for full and partial layer winding scenarios.

Table I
WINDING SPECIFICATION OF PROTOTYPE 1 AND 2

	Primary	Secondary	
		P1	P2
Number of full layers m	2	2	2
Turns of full layer t	16	16	16
Number of partial layers	0	0	1
Turns of partial layer t_0	0	0	10
Winding diameter	1.56 mm	1.56 mm	1.56 mm

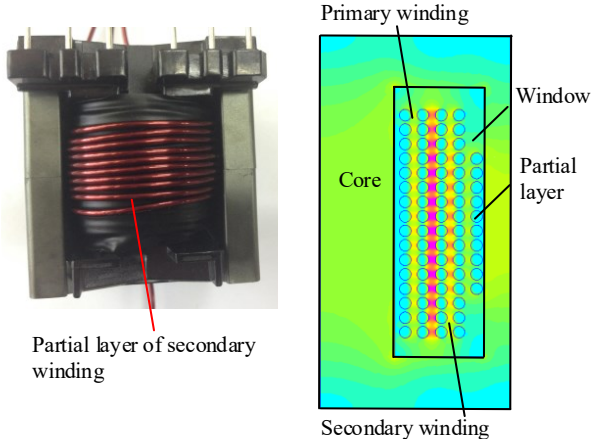

Figure 8. Photo of Prototype 2 and its FEM simulation model.

B. Finite Element Modeling and Experimental Verification

For the verification of the derived equation, two transformers are built, named Prototype 1 (P1) and Prototype 2 (P2), with the same primary winding and different secondary windings. The winding specification is given in table I.

Prototype 1 is with a full secondary winding and Prototype 2 is with a partial secondary winding. All of the prototypes are with the EPCOS PQ50/50 core and same isolation. The ac resistances are measured by Aglient E5061B network analyzer. Prototype 2 and its Finite Element Method (FEM) simulation model are shown in Fig. 8.

The results shown in Fig. 9 reveal a well agreement among the analytical, simulation, and experimental results. The large diameter of the conductor leads to the large penetration

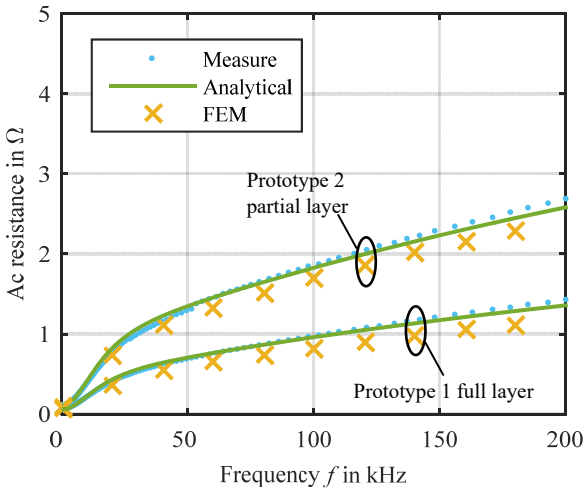

Figure 9. The analytical, simulation, and experimental results of the ac resistance of Prototype 1 and 2 under different frequency (i.e., different penetration ratio).

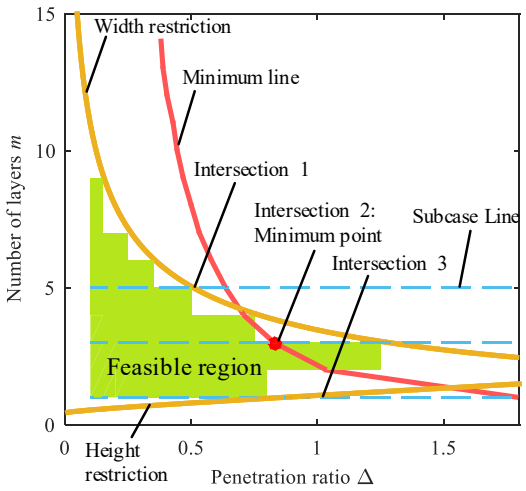

Figure 10. Transformer winding design map with partial layer.

ratio Δ. It results in the large skin and proximity effects coefficients υ_3 and υ_2 in (18). So the difference between Prototype 1 and Prototype 2 is quite high and increases with the frequency. The difference almost equals to the ac resistance of Prototype 1 in 200 kHz. It indicates that in high-power and high frequency range, the introduction of ac resistance formula for the partial layer is necessary.

IV. Optimal Winding Design with Partial Layers

For winding arrangement with m full layers and one partial layer, the previously discussed core window width and height boundary are still valid and can be modified to:

$$d_{\mathrm{c}} \geq (m+1)d_{\mathrm{opt}} + 2(m+1)d_{\mathrm{iso}} + md_{\mathrm{wwiso}} + 2d_{\mathrm{cwiso}}, \quad (22)$$

$$h_{\mathrm{c}} \geq td_{\mathrm{opt}} + 2td_{\mathrm{iso}} + (t-1)h_{\mathrm{wwiso}} + 2h_{\mathrm{cwiso}}. \quad (23)$$

In partial layer scenario, t is calculated by:

$$t = \frac{N - t_0}{m}. \quad (24)$$

When N is an even number, there are N/2 kinds of t_0 (i.e., 0, 1, 2, ..., N/2-1). When N is an odd number, there are $(N+1)$/2 kinds of t_0. Each kind of t_0 is corresponding to a height boundary restricted by (23).

Additionally, there is a layer boundary ensuring that t_0 does not exceed t: t_0<t. By substituting (24) into the boundary, the restriction is the function of m:

$$m < \frac{N}{t_0} - 1. \quad (25)$$

A design map for N= 16 and t_0= 1 is given in Fig. 10 for illustration, which is almost the same shape like Fig. 4. In this sub-situation, the number of turns left for full layer is 15. Therefore, there are three kinds of combination for the (m, t) pair: (1, 15), (3, 5), and (5, 3). Each pair is related to a subcase line in Fig. 10, which is in blue and parallel to the x-axis. The y coordinate value of the subcase line indicates the related number of layers, which is 1, 3, and 5, respectively. The parts of the subcase line in the feasible region are all of the viable scenarios in the sub-situation. The minimum resistance point of each layer is its intersection of the yellow boundary line or the pink minimum line, depending on the position of the boundary and the minimum line. The points are marked with intersection 1 to 3. By comparing the minimum points of each layer, the overall minimum point in the design map can be obtained. In this situation, intersection 2 is the minimum point marked with red point. The global minimization resistance point is obtained by comparing the minimum points in all of the design maps.

The winding design method above is for core window with one winding, which is for inductor application. It is also applicable to transformer with primary and secondary windings. As the balance of delivered power, the same window area is preferred for the primary and secondary winding, which means the half width for each winding. The porosity factor modification in (21) can also be integrated into the proposed design method to get a more precise design result.

A transformer for the 20 kHz LCC resonant circuit is designed with this method, the partial layer is preferred to accurately meet the requirements of number of total turns N, the core is PQ50/50, both the core and isolation restriction is given in table II and all of the variables can be found in (8) and (9). m is considered as a design variable.

The resultant winding design is given in table III. The measured results of the designed transformer is illustrated in Fig. 11. For comparison, a full layer transformer with 2 layers 0.25 mm diameter round conductors as the secondary side is also studied. Other parameters are kept the same, and the winding dimension is also within the design restrictions. It can be noted that the optimized winding has a 24.85 % ac resistance reduction compared to this alternative designed one at 20 kHz. In fact, any other design solutions within the design restriction map in Fig. 4 will have a higher ac resistance compared to the optimum design point. The measured ac

Table II
WINDING DESIGN INPUTS OF ISOLATION AND CORE SIZE

	p	d_{wwiso}	d_{cwiso}	h_{wwiso}	h_{cwiso}	h_{c}	d_{c}
Primary side	0.33	1.2 mm	1.2 mm	0.2 mm	2.0 mm	36.1 mm	5.5 mm
Secondary side	0.33	1.2 mm	1.2 mm	0.2 mm	2.0 mm	36.1 mm	5.5 mm

Table III
WINDING DESIGN OUTPUTS

	Primary	Secondary
Number of total turns N	14	34
Number of full layers m	1	1
Turns of full layer t	14	22
Number of partial layers	0	1
Turns of partial layer t_0	0	12
Winding diameter output	0.9966 mm	0.5703 mm
Winding diameter chosen	1.0400 mm	0.6200 mm
Ac resistance at 20 kHz	0.0280 Ω	0.2094 Ω
Total ac resistance reflected to primary	0.0635 Ω	

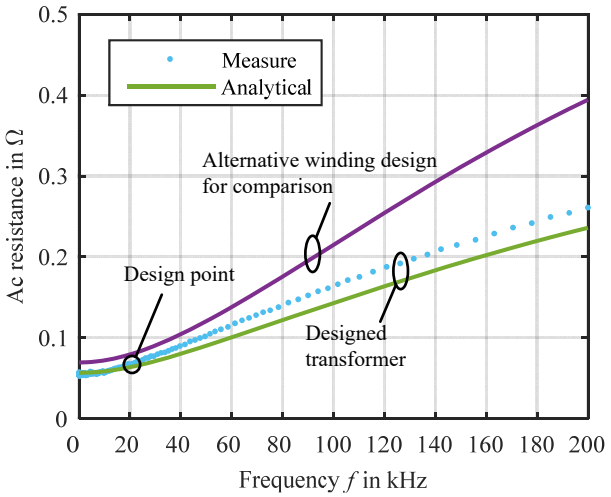

Figure 11. Experimental result of the designed transformer with optimum winding losses.

resistance reflected to the primary side is 0.0665 Ω at 20 kHz, with a difference of 4.55% only, compared to the analytical results. The results verify both the proposed partial layer ac resistance model and the optimal design of the winding with partial layer in terms of ac resistance.

V. CONCLUSIONS

An ac resistance optimization method is proposed and experimentally verified in this paper for inductor and transformer winding design. With a derived analytical equation for ac resistance of windings with partial layers, the proposed method is applicable for the winding optimization with partial layers as well. Two transformer prototypes have been built and the analytical, FEM simulation, and experimental results show a well agreement with each other. A transformer winding design case for a LCC converter is discussed. It results in a 24.85 % ac resistance reduction at the frequency of interest with the proposed optimization method, compared to an alternative design.

APPENDIX A
DERIVATION OF THE PARTIAL LAYER WINDING LOSSES

With the one dimensional flux assumption in section (II-A) and the Maxwell equations, the magnetic field intensity H_z is described by a second-order ordinary differential equation:

$$\frac{\mathrm{d}^2 H_z}{\mathrm{d}\, y^2} = j\sigma\omega\mu H_z = \alpha^2 H_z, \tag{26}$$

with:

$$\alpha = \frac{1+j}{\delta}. \tag{27}$$

The boundary condition of the internal magnetic field strengths is explained in (16) and rewritten here:

$$H'_{\mathrm{int1}} = -H'_{\mathrm{int2}} = \frac{k\hat{I}}{2h_{\mathrm{c}}}. \tag{28}$$

According to (26), the solution of magnetic field strength for skin effect in z direction H'_{sz} decreases with the ratio k:

$$H'_{\mathrm{sz}} = \frac{k\hat{I}\sinh\alpha y}{2h_{\mathrm{c}}\sinh\frac{\alpha d_{\mathrm{w}}}{2}}. \tag{29}$$

And so as the skin effect current density in x direction J'_{sx}:

$$J'_{\mathrm{sx}} = \frac{\mathrm{d}\, H'_{\mathrm{sz}}}{\mathrm{d}\, y} = \frac{\alpha k\hat{I}\cosh\alpha y}{2h_{\mathrm{c}}\sinh\frac{\alpha d_{\mathrm{w}}}{2}}. \tag{30}$$

The skin effect losses for the $(m+1)th$ partial layer winding is:

$$P'_{\mathrm{s}} = t_0\frac{l_{\mathrm{w}}\frac{h'_{\mathrm{w}}}{t_0}}{2\sigma}\int_0^{d_{\mathrm{w}}}|J'_{\mathrm{sx}}|^2\,\mathrm{d}\, y = \frac{k\hat{I}^2}{4h_{\mathrm{c}}\sigma\delta}\nu_1, \tag{31}$$

where

$$\nu_1 = \frac{\sinh\triangle+\sin\triangle}{\cosh\triangle-\cos\triangle}, \tag{32}$$

l_{w} is the one turn length of conductor.

The outside external magnetic field strength of the partial layer increases $\frac{k\hat{I}}{h_{\mathrm{c}}}$ instead of $\frac{\hat{I}}{h_{\mathrm{c}}}$, which leads to the averaged external magnetic field strength boundary condition become:

$$H'_{\mathrm{ext1}} = H'_{\mathrm{ext2}} = \frac{\frac{m\hat{I}}{h_{\mathrm{c}}}+\frac{m\hat{I}+k\hat{I}}{h_{\mathrm{c}}}}{2} = \frac{2m\hat{I}+k\hat{I}}{2h_{\mathrm{c}}}. \tag{33}$$

The external magnetic field strength for proximity effect in z direction H'_{pz} can be solved by substituting $H'_{\mathrm{ext1}} = H'_{\mathrm{ext2}}$:

$$H'_{\mathrm{pz}} = \frac{\cosh \alpha y}{\cosh \frac{\alpha d_{\mathrm{w}}}{2}} H'_{\mathrm{ext1}}. \tag{34}$$

The induced current density of the $(m+1)th$ layer is:

$$J'_{\mathrm{px}} = \frac{\mathrm{d}\, H'_{\mathrm{pz}}}{\mathrm{d}\, y} = \frac{\alpha \sinh \alpha y}{\cosh \frac{\alpha d_{\mathrm{w}}}{2}} H'_{\mathrm{ext1}}. \tag{35}$$

The proximity effect losses for the $(m+1)th$ partial layer winding is determined by:

$$\begin{aligned} P'_{\mathrm{P}} &= t_0 \frac{l_{\mathrm{w}} \frac{h'_{\mathrm{w}}}{t_0}}{2\sigma} \int_0^{d_{\mathrm{w}}} |J'_{\mathrm{px}}|^2 \,\mathrm{d}\, y \\ &= \frac{k l_{\mathrm{w}} \hat{I}^2 (2m+k)^2}{4 h_{\mathrm{c}} \sigma \delta} \nu_2, \end{aligned} \tag{36}$$

where

$$\nu_2 = \frac{\sinh \triangle - \sin \triangle}{\cosh \triangle + \cos \triangle}. \tag{37}$$

By adding the losses of m full layers P_{m} and the skin and proximity losses of the partial layer, the total losses are:

$$\begin{aligned} P &= P_{\mathrm{m}} + P'_{\mathrm{s}} + P'_{\mathrm{p}} \\ &= \frac{l_{\mathrm{w}} \hat{I}^2}{h_{\mathrm{c}} \sigma \delta} \left(\frac{m}{4} \nu_1 + \frac{4m^3 - m}{12} \nu_2 + \frac{k}{4} \nu_1 + \frac{k(2m+k)^2}{4} \nu_2 \right). \end{aligned} \tag{38}$$

With the following mathematical identities:

$$\frac{\nu_1 + \nu_2}{2} = \frac{\sinh(2\triangle) + \sin(2\triangle)}{\cosh(2\triangle) - \cos(2\triangle)} = \nu_3, \tag{39}$$

(38) can be expressed with more common form:

$$\begin{aligned} P =& \frac{l_{\mathrm{w}} \hat{I}^2}{h_{\mathrm{c}} \sigma \delta} \frac{(m+k)}{2} \nu_3 \\ &+ \frac{l_{\mathrm{w}} \hat{I}^2}{h_{\mathrm{c}} \sigma \delta} \frac{4m^3 - 4m - 3k + 3k(2m+k)^2}{12} \nu_2. \end{aligned} \tag{40}$$

The ac resistance of the total winding is determined by:

$$\begin{aligned} R_{\mathrm{ac}} =& \frac{m+k}{h_{\mathrm{w0}} \sigma \delta} l_{\mathrm{w}} t \nu_3 \\ &+ \frac{4m^3 - 4m - 3k + 3k(2m+k)^2}{6 h_{\mathrm{w0}} \sigma \delta} l_{\mathrm{w}} t \nu_2. \end{aligned} \tag{41}$$

The dc resistance of $m+1$ layers rectangle winding is:

$$R_{\mathrm{dc}} = \frac{(mt + t') l_{\mathrm{w}}}{h_{\mathrm{w0}} \sigma d_{\mathrm{w}}} = \frac{t(m+k) l_{\mathrm{w}}}{h_{\mathrm{w0}} \sigma d_{\mathrm{w}}}. \tag{42}$$

Thus the ac resistance factor for rectangle conductor can be expressed by:

$$F_{\mathrm{r}} = \Delta \nu_3 + \frac{4m^3 - 4m - 3k + 3k(2m+k)^2}{6(m+k)} \Delta \nu_2. \tag{43}$$

For square conductors, the derivation process is almost the same except that the height of the conductor is equal to the width:

$$h_{\mathrm{w0}} = d_{\mathrm{w}}, \tag{44}$$

and the related ac resistance factor is also the same.

For round conductors, (43) is also valid by transferring the diameter d to equivalent d_{w} with (5).

REFERENCES

[1] I. Villar, *Multiphysical characterization of medium-frequency power electronic transformers*. Lausanne, Switzerland: École Polytechnique Fédérale de Lausanne, 2010.

[2] J. Muehlethaler, *Modeling and multi-objective optimization of inductive power components*. Zurich, Switzerland: Eidgenössische Technische Hochschule Zürich, 2012.

[3] J.-P. Vandelac and P. Ziogas, "A novel approach for minimizing high-frequency transformer copper losses," *IEEE Trans. Power Electron.*, vol. 3, no. 3, pp. 266–277, Jun. 1988.

[4] C. Sullivan, "Optimal choice for number of strands in a litz-wire transformer winding," *IEEE Trans. Power Electron.*, vol. 14, no. 2, pp. 283–291, Mar. 1999.

[5] P. Dowell, "Effects of eddy currents in transformer windings," in *Proc. Inst. Electr. Eng.*, vol. 113, Aug. 1966, pp. 1387–1394.

[6] J. Ferreira, "Improved analytical modeling of conductive losses in magnetic components," *IEEE Trans. Power Electron.*, vol. 9, no. 1, pp. 127–131, Jan. 1994.

[7] J. Lammeraner and M. Štafl, *Eddy currents*. London, U.K.: Iliffe, 1966.

[8] M. K. Kazimierczuk, *High-frequency magnetic components*. West Sussex, U.K.: John Wiley & Sons, 2009.

[9] V. Vaisanen, J. Hiltunen, J. Nerg, *et al.*, "Ac resistance calculation methods and practical design considerations when using litz wire," in *Proc. IEEE 39th Annual Conf. Ind. Electron. Soc.*, Nov. 2013, pp. 368–375.

[10] C. Sullivan, "Computationally efficient winding loss calculation with multiple windings, arbitrary waveforms, and two-dimensional or three-dimensional field geometry," *IEEE Trans. Power Electron.*, vol. 16, no. 1, pp. 142–150, Jan. 2001.

[11] W. G. Hurley and W. H. Wölfle, *Transformers and inductors for power electronics: Theory, design and applications*. West Sussex, U,K.: John Wiley & Sons, 2013.

[12] R. Wojda and M. K. Kazimierczuk, "Winding resistance of litz-wire and multi-strand inductors," *IET Power Electron.*, vol. 5, no. 2, pp. 257–268, Feb. 2012.

[13] K. V. Iyer, K. Basu, W. P. Robbins, *et al.*, "Determination of the optimal thickness for a multi-layer transformer winding," in *Proc. IEEE Energy Convers. Congr. Expo.*, Sep. 2013, pp. 3738–3741.

[14] M. Kaymak, Z. Shen, and R. W. D. Doncker, "A new winding design method for inductors and transformers," in *Proc. IEEE Wksp. Control Model. Power Electron.*, Jun. 2016, pp. 1–7.